1968

Isotope effect of interstitial diffusion of carbon in a dilute Fe-Si alloy

Edward T. Yen

ISOTOPE EFFECT
OF
INTERSTITIAL DIFFUSION OF CARBON
IN A DILUTE FE-SI ALLOY

BY

EDWARD T. YEN, 1941

A

THESIS

submitted to the faculty of the

UNIVERSITY OF MISSOURI - ROLLA

in partial fulfillment of the requirements for the

Degree of

MASTER OF SCIENCE IN METALLURGICAL ENGINEERING

Rolla, Missouri

1968

Approved by

H. L. Otts (Advisor) 6-14-68

J B Clark 6-14-68

ABSTRACT

The isotope effect of carbon interstitial diffusion in a Fe-2.75at%Si alloy has been measured at -3.10°C using the disaccommodation technique. The disaccommodation has been analyzed in terms of two relaxation processes which are discussed on the basis of the reorientation mechanism of carbon interstitials at Fe-Fe sites and Fe-Si sites respectively. The ratios of the relaxation times τ_{13}/τ_{12} are 1.0382 for the former and 1.0072 for the latter relaxation process. This result is discussed on the basis of many-body reaction rate theory.

ACKNOWLEDGEMENT

The author would like to express his deep appreciation to his thesis advisor Professor Manfred Wuttig for his guidance in all phases of his graduate work. His stimulating discussions and invaluable assistance have made this thesis possible.

The author is also indebted to Mr. Robert Crosby of the U.S. Bureau of Mines for melting and analyzing the Fe-Si ingot alloy used in this investigation and to Miss Teresa Chi for preparing this manuscript.

TABLE OF CONTENTS

Page

LIST OF FIGURES

Page

Figures

LIST OF TABLES

Page

Table

I. INTRODUCTION AND LITERATURE REVIEW

A. Magnetic Aftereffects Due to Interstitials

Ever since the discovery (1) that minute amounts of either nitrogen or carbon are capable of producing elastic and magnetic aftereffects in iron, studies of both magnetic and elastic aftereffects have been carried out extensively (2).

In 1941, a detailed theory of the magnetic aftereffect on an atomic basis was developed by Snoek (3,4). He assumed that the magnetostrictive strains were the physical basis. In 1952, Neel argued that there was direct coupling between the interstitial and the spontaneous magnetization which was more important than the magnetostrictive strains (5,6). This coupling has been explained as the electronic spin-orbit interaction of the 3d orbit electrons of the iron atom (7,8). Especially, it was shown that the electron interaction energy was much greater than the magnetostrictive energy in the dilute iron carbon or iron nitrogen alloys (9).

B. Magnetic Aftereffects in Binary Iron-Base Alloys

1. Substitutional-Iron-Base Alloys

Measurements of the time dependence of the initial magnetic permeability, the disaccommodation, have been applied to study the behavior in Fe-Si alloys. A disaccommodation occurring at around 400°C was reported (10,11). Two kinds of explanations for this type of

disaccommodation were forwarded:

a. Reorientation of silicon pairs (Zener relaxation) with respect to the spontaneous magnetization (12,13).

b. Long range diffusion of continuously migrating vacancies to sinks and/or sources into Bloch walls (14,15).

By investigating the dependence of the disaccommodation on silicon content (10,13) and the stabilization field (11), it was concluded that the Zener mechanism was the more likely of the two.

2. Interstitial-Substitutional-Iron-Base Alloys

It is known that additional internal friction peaks adjacent to the normally existing Snoek peak are due to the diffusion controlled reorientation of the interstitials located next to the substitutionals (12-18). While the extra internal peaks found at temperatures above the Snoek peak were interpreted as due to the reorientation of interstitials located next to the one substitutional, peaks found at temperatures below the Snoek peak were interpreted as due to the reorientation of the interstitials located next to substitutional pairs (19,20). The equivalent disaccommodations have been found in Fe-Si-C (21), Fe-Mn-N, Fe-Cr-N, Fe-V-N and Fe-Ti-N alloys (22).

C. Isotope Effect of Diffusion

1. Substitutional Binary Alloys

Measurements of the isotope effect of diffusion have been reported for various substitutional binary alloys such as Ni_{58}, Ni_{60} & Ni_{62} in Cu (23), Fe_{55} & Fe_{59} in Ag (24), Cd_{115} & Cd_{109} in Ag, Cu (25), Na_{22} & Na_{24} in NaCl (26), Li_6 & Li_7 in Si and W (27,28). The investigations have generally shown that the jump frequency is proportional to the inverse square root of the mass of the diffusing isotope. The explanation was commonly based on conventional classical theory of absolute reaction rates (29). The many-body aspects of the diffusion problem as introduced by Vineyard (30) were considered as a correction to the above oversimplified reaction rate theory.

In Vineyard's theory, the diffusion process was considered as the motion of a representative point over a potential barrier in the N-dimensional phase space of the crystal containing N/3 atoms. The jump frequency Γ of one diffusing element is then given by:

$$\Gamma = \frac{C''}{\gamma} = \frac{C'}{\sqrt{m^*}} \text{ EXP } [-(\phi(P)-\phi(A))/kT] \qquad (1)$$

where

$$m^* = \sum_{i=1}^{N} m_i c_i^2 \qquad (2)$$

and Γ - jump freqnency

m^* - effective mass

T - absolute temperature

k - Boltzmann's constant

$\phi(P)-\phi(A)$ - activation energy

τ - average relaxation time

C',C" - constants

and c_i is a direction cosine between the normal of the hyper-surface and the coordinate axis x_i of the diffusing i^{th} species. The hyper-surface is defined as a configuration surface that passes through the saddle point between two adjacent minimum potential equilibrium sites and is perpendicular to the potential energy contour everywhere. The mass to be associated with the x_i axis is m_i. This analysis showed that the jump frequency is proportional to $(m^*)^{-\frac{1}{2}}$, where m* is an effective mass, the value of which is bound by the smallest and largest masses in the entire system.

Rice et al (31-34) have also examined the many-body aspects using classical dynamics instead of Vineyard's thermodynamic approach. The treatment differed from that of Vineyard in that the assumption of an equilibrium state at the top of the potential barrier was removed. However, so far it has not been possible to use this dynamic model to calculate the mass effect on the many-body aspects on any realistic basis.

2. Binary Alloys with Interstitials

The isotope effect of interstitial diffusion in binary alloys has not yet been investigated. It was reported that the isotope effect of the carbon interstitials in the pure iron behaved according to the conventional reaction rate theory (35). The ratio δ of relaxation times τ_{13}/τ_{12} of

the samples one containing C_{13} and the other C_{12} is equal to the ratio of the square root of the mass of C_{13} and C_{12}, 1.044 .

The present investigation is an attempt to determine the isotope effect of interstitial diffusion in binary alloys. The isotopes chosen for this experiment were C_{13} and C_{12}, and the host polycrystal, Fe-Si. Disaccommodation rather than anelastic techniques were used because of the superior sensitivity of the former as can be seen by comparing the extra disaccommodation (21) and the extra internal friction peaks (17) of a Fe-6at%Si-.05at%C alloy. The carbon isotopes were selected for the following reasons: (1) the study of the disaccommodation of these isotopes permitted a careful re-examination of the carbon isotope effect in the Fe-Fe sites; (2) the extra disaccommodation to be utilized in this study is known to exist in Fe-Si-C alloys (21); (3) neither carbon isotope is radioactive and thus both could be handled easily.

II. EXPERIMENTAL PROCEDURE

A. Permeability Measurement and Apparatus

The initial magnetic permeability measurements were performed using a self balancing a.c. bridge (Fig. 1). With the mutual inductance coil containing the specimen as a core, the disaccommodation defined as the change of the permeability with respect to time of the Fe-Si-C specimen could be measured with a precision of 3 parts in 10^5 using a measuring field of 7 mOe and a bridge frequency of 220 cps. Through the lock-in amplifier and tuned control loop, the amplified unbalanced signal from the inductance coil was fed into a recorder which adjusted a bridge to rebalance the signal. The earth magnetic field was kept from the specimen and the inductance coil by shielding it with a double layer of nickel sheets.

In order to randomize the domain boundary configuration the specimens were demagnetized before each disaccommodation run by sweeping an a.c. 60 cycle field from 50 Oe to 1 mOe through a coil around the inductance coil for several relaxation times. The demagnetization procedure did not disturb the thermal equilibrium of the specimen.

As the permeability is temperature dependent and, more important, the expected isotope effects is small, the temperature control requirements were very stringent. For instance, a temperature change of 0.1 degree would cause a change of the relaxation time of 2%, which is of the order of magnitude of the expected isotope effect.

Fig. 1

Schematic diagram of disaccommodation measuring apparatus

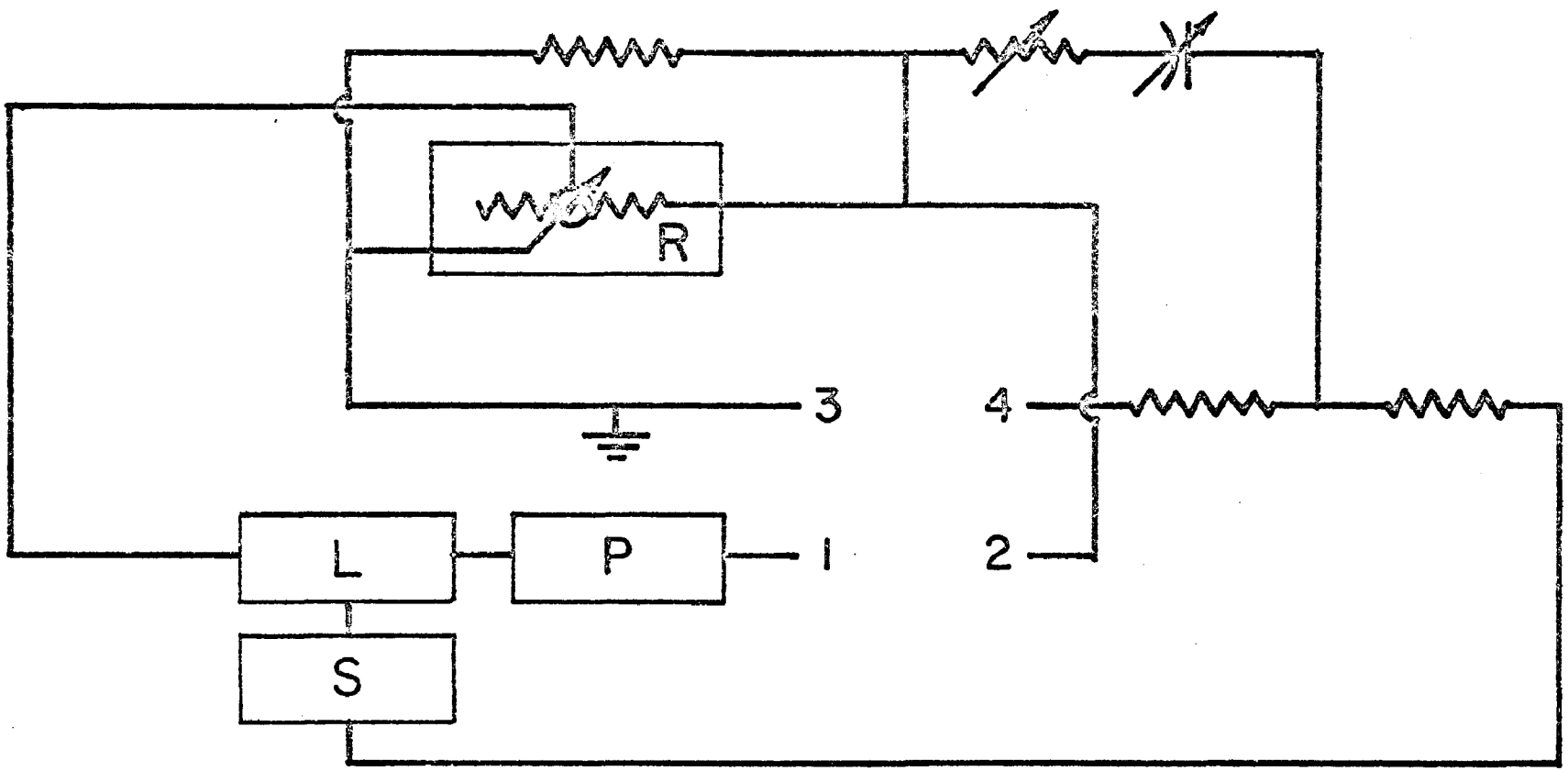

S OSCILLATOR L LOCKIN AMPLIFIER

R RECORDER P PREAMPLIFIER

Fig. 1

Fig. 2 shows the furnace and the temperature control circuit. The furnace, made of an Aluminum alloy, was wound noninductively with resistance wire. It was operated by a low voltage (less than 40 volts) high current (up to 30 amps.) d.c. power supply. At the ends on both sides of the furnace, two pyrex glass plates were installed to minimize heat losses. The furnace was placed in the center of a freezer (8 cubic feet) and was controlled by a proportional-rate-repeat-approach adjusting type temperature controller. This arrangement allowed the temperature to be controlled to within the limit of detection of $\pm 0.025^{\circ}C$ at $0^{\circ}C$ with a temperature gradient along the 1 3/4 inch specimen length of less than $0.05^{\circ}C$. This temperature gradient does not affect the measurement of the isotope effect as the nearly identical C_{13} and C_{12} specimens were placed in the same location for the disaccommodation measurements.

B. Specimen Preparation

The ingot was prepared by inductively melting of Armco iron 99.0% Fe and silicon 99.9% Si with charge ratio 99.495 Fe to 1.531 Si in an MgO crucible at Helium atmosphere at -5" Hg pressure. The analysis showed 1.4wt% (2.75at%) Si content. The ingot specimen was swaged into rods of 0.1038 inch diameter. The specimens were annealed simultaneously at $800^{\circ}C$ in wet hydrogen for 24 hrs. followed by another anneal of 10 hrs. in dry hydrogen in order to reduce the carbon, nitrogen and oxygen contents.

Fig. 2

Furnace and temperature control system

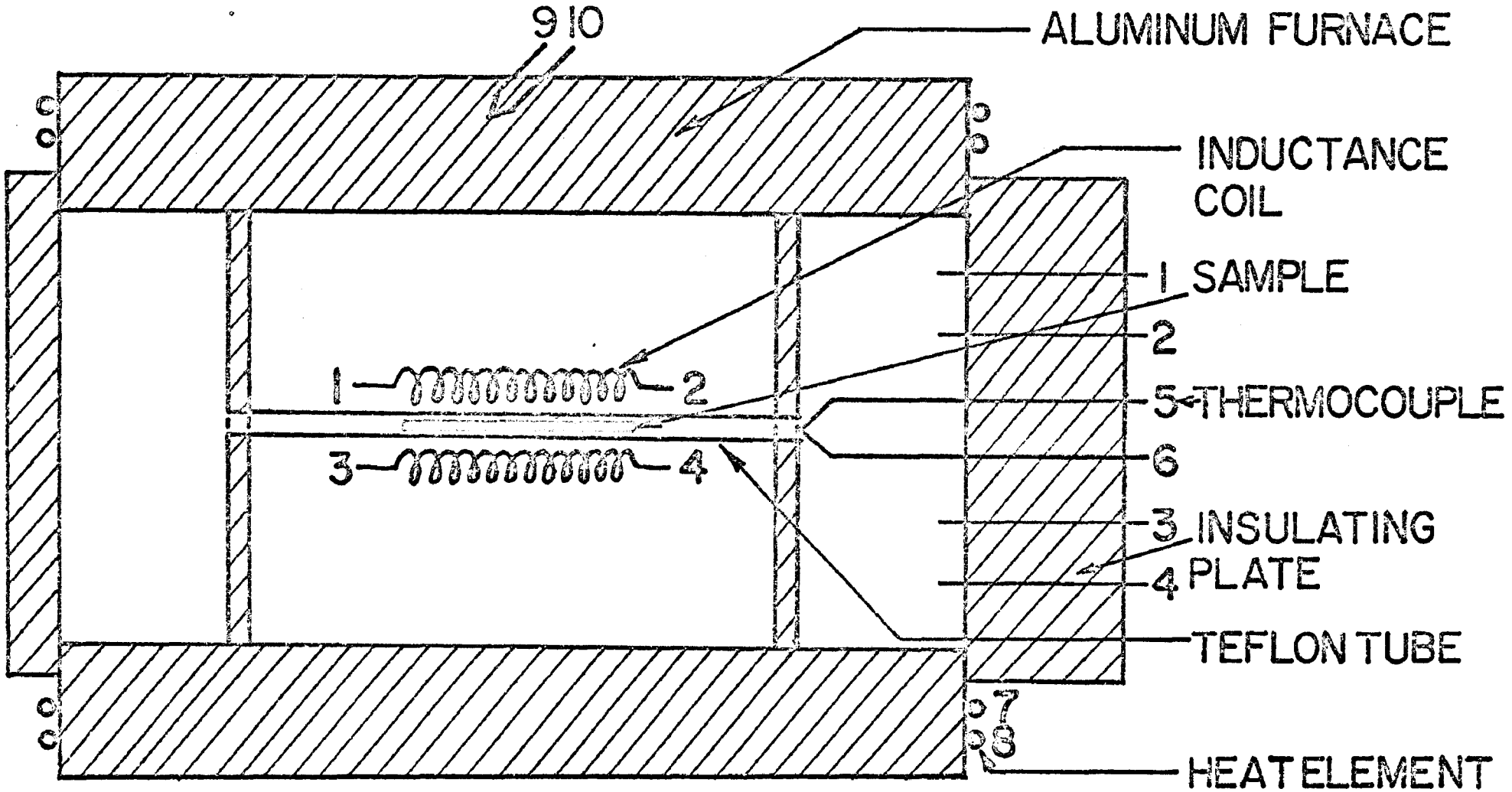
9 10
ALUMINUM FURNACE
INDUCTANCE COIL
1 SAMPLE
2
5 THERMOCOUPLE
6
3 INSULATING PLATE
4
TEFLON TUBE
7
8
HEAT ELEMENT
1
2
3
4

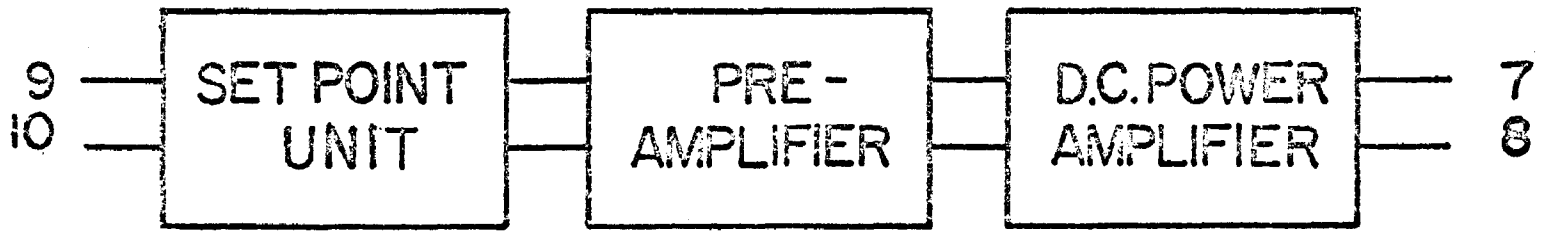
9
10
SET POINT UNIT
PRE-AMPLIFIER
D.C. POWER AMPLIFIER
7
8

Fig. 2

Two kinds of methane were used for the carburization of two identical specimens chosen from the above lot. Methane with C_{12} (98.9% C_{12} and 1.1% C_{13}) and methane with C_{13} (93.9% C_{13} and 6.1% C_{12}) were mixed with pure dry hydrogen at the same ratio (14% CH_4 to 86% H_2) for both carburizations. The two specimens were carburized separately with the above isotope gas mixtures in a sealed quartz chamber at the same temperature (800°C) for the same period of time (8 hrs.). This carburization treatment resulted in a carbon content about 0.015 weight percent as estimated from Smith's and Darken's data (36,37). The specimens were quenched directly from the chamber into a brine solution. The quenching rates were of the order of 10^3 deg/sec. No phase transformation or surface oxidation was observed.

III. EXPERIMENTAL RESULTS AND DATA ANALYSIS

A. Disaccommodation Measurement

The disaccommodation measurements on a Fe-C_{12} and a Fe-Si-C_{12} specimen carried out between -20°C and 10°C at 1 min. and 10 min. are shown in the Fig. 3 . By comparing the two curves in this Figure, it can be seen that the disaccommodation in the Fe-Si-C_{12} specimen above -5°C was predominantly due to the disaccommodation of carbon interstitials located near to silicon substitutionals i.e. in Fe-Si sites. Consequently, the temperature region for the most sensitive disaccommodation measurements of the carbon-silicon pairs was between -5°C and 0°C.

No history dependence of the disaccommodation measurements was observed during the heating and cooling cycles in the -20°C to 10°C range. This indicated that no precipitation of carbon occurred in this temperature range within the period of observation.

The disaccommodation of the Fe-Si-C_{12} and Fe-Si-C_{13} was measured at exactly the same temperature of -3.10°C from 0.5 min. until 50 min. and 60 min. respectively. The disaccommodation curves, taken from the self-balance recorder, were converted into reluctivity change R (see next paragraph for definition) versus time as shown in Fig. 4 and Fig. 5 .

B. Data Analysis

All data analysis was accomplished by Fortran IV

Fig. 3

Normalized reluctivity difference ΔR versus temperature θ for Fe-2.75at%Si-C and Fe-C alloys

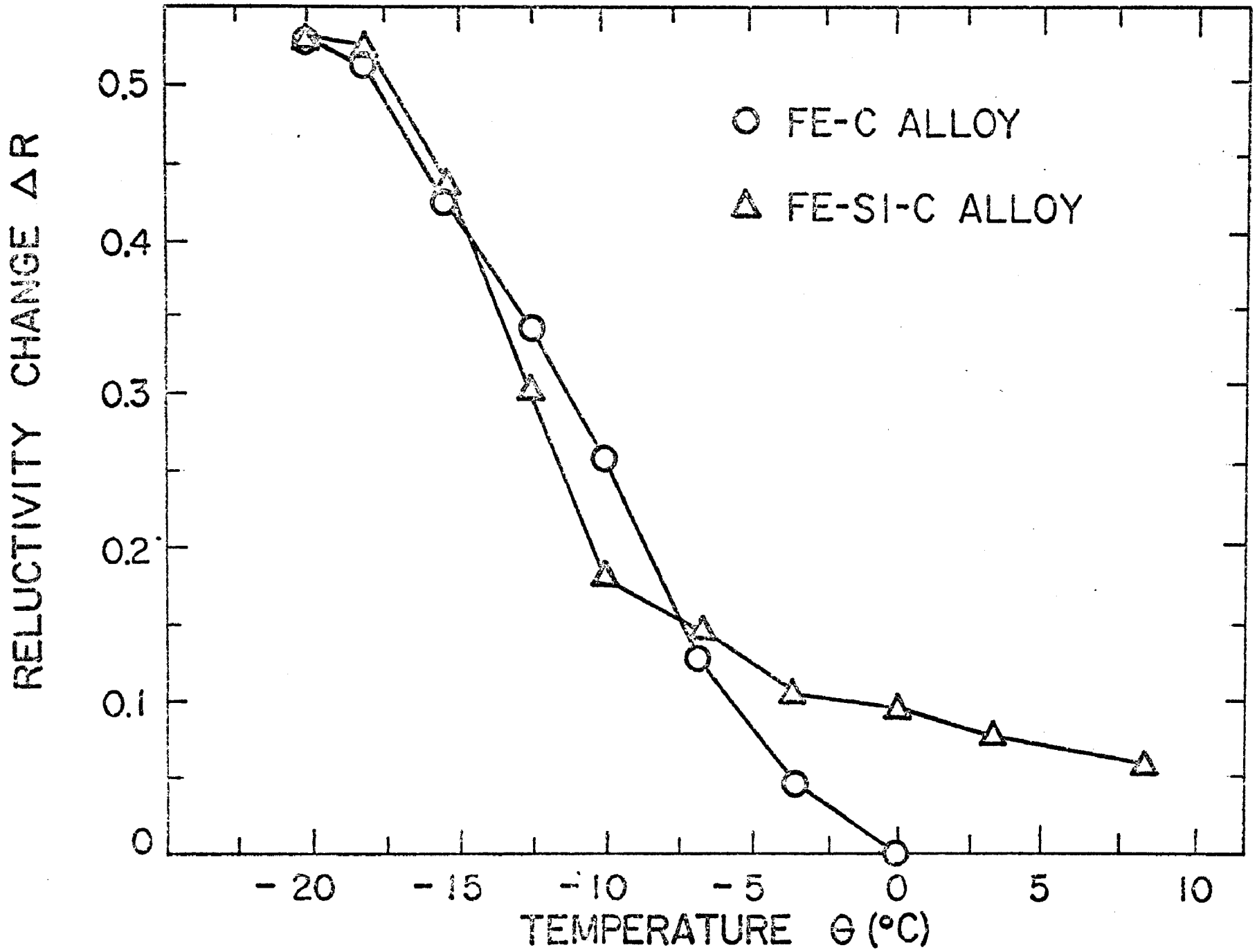
RELUCTIVITY CHANGE ΔR
0.5
0.4
0.3
0.2
0.1
0
FE-C ALLOY
FE-SI-C ALLOY
-20
-15
-10
-5
0
5
10
TEMPERATURE θ (°C)

Fig. 3

Fig. 4

Isothermal relaxation of the logrithmic reluctivity change LOG R versus time t of Fe-2.75at%Si-C_{12} alloy at -3.10°C

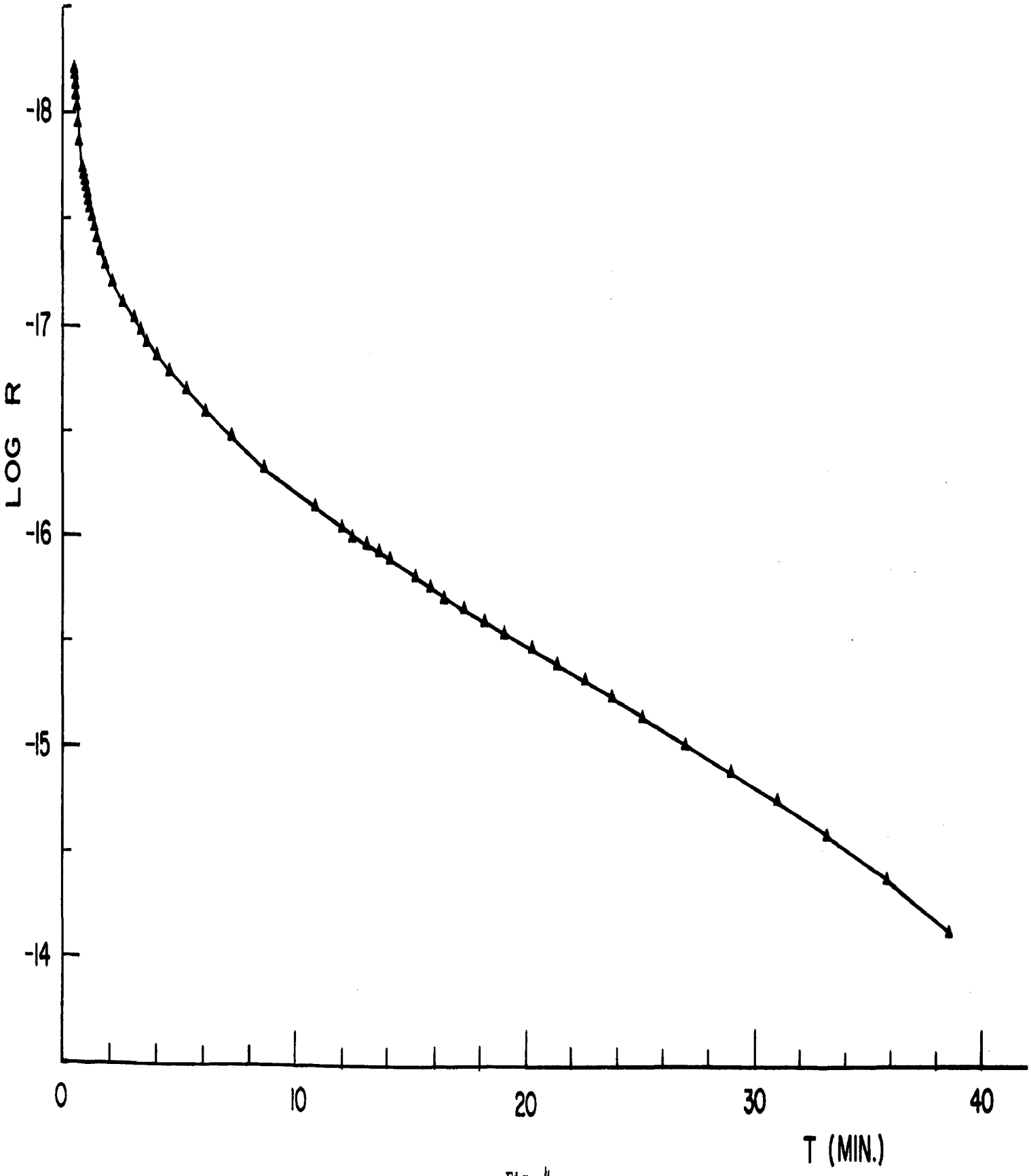

Fig. 4

Fig. 5

Isothermal relaxation of the logrithmic reluctivity change LOG R versus time t of Fe-2.75at%Si-C_{13} alloy at -3.10°C

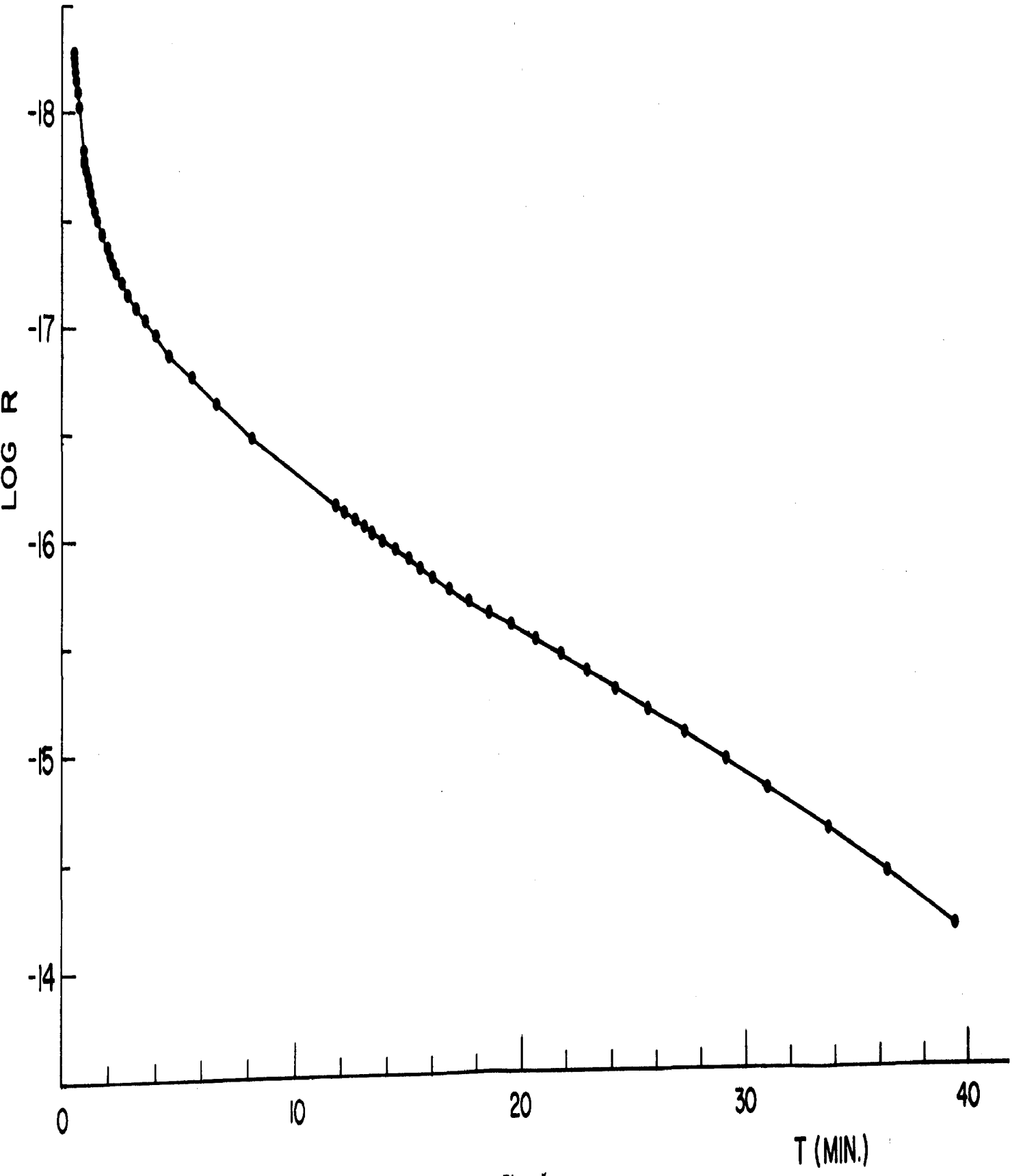

Fig. 5

programming on the IBM 360 computer. A sample program is shown in the Appendix.

1. Sum of Exponential Analysis

The isothermal permeability data were analyzed as a sum of first order relaxation processes (35):

$$R = \frac{1}{\mu(\infty)} - \frac{1}{\mu(t)} = \sum_j a_j \text{ EXP } (-t/\tau_j) \qquad (3)$$

where $\frac{1}{\mu(t)}$ - inverse permeability, i.e., reluctivity

t - time

τ_j - the relaxation time of the j^{th} relaxation

a_j - the relaxation strength of the j^{th} relaxation

and

$$\sum_j a_j = \frac{1}{\mu(\infty)} - \frac{1}{\mu(0)} \quad .$$

The curve fitting of the data points with respect to the above nonlinear equation was programmed according to the method described by Draper and Smith (38). This method allowed the number of relaxations, the relaxation strengths, and the relaxation times to be adjusted to obtain a best least square fit.

The results of these analyses show that with two relaxation stages, the ratio of the first stage relaxation times $\delta_1 = \tau_{13,1}/\tau_{12,1}$ is 1.0412 and that of the second stage relaxation times $\delta_2 = \tau_{13,2}/\tau_{12,2}$ is equal to 1.0152 . The results are also displayed in Table 1 . It is noted that δ_1 agrees well with Bosman's results (35) who obtained for the ratio of the relaxation times of Fe-C_{13}

Table 1

Computed results of the sum of exponential analysis, lognormal analysis and lognormal analysis with constraint

Table 1

Mode of Analysis	β_1	β_2	$\tau_{13,1}$ [min]	$\tau_{12,1}$ [min]	$\tau_{13,2}$ [min]	$\tau_{12,2}$ [min]	δ_1	δ_2	*VAR$_{13}$	*VAR$_{12}$
Single Exponentials	0	0	0.545	0.523	10.047	9.897	1.0412	1.0152	2.321	2.394
Lognormal Analysis	0.6	0.8	0.410	0.395	8.549	8.468	1.0373	1.0095	1.646	1.868
	0.6	1.0	0.382	0.368	7.593	7.541	1.0366	1.0069	1.242	1.288
	0.6	1.2	0.351	0.339	6.555	6.542	1.0368	1.0048	1.919	2.233
Lognormal Analysis with Constraint	0.6	0.75	0.417	0.401	8.770	8.678	1.0382	1.0106	1.701	1.900
	0.6	1.0	0.382	0.368	7.597	7.538	1.0382	1.0077	1.267	1.290
	0.6	1.25	0.344	0.331	6.293	6.262	1.0382	1.0048	1.899	2.241

* VAR - the relative variance is the sum of squares about the regression

to Fe-C_{12} 1.044 .

The absolute value for the relaxation time of the carbon interstitials in Fe-Fe sites (first stage) agrees well with previously published data. The relaxation time for carbon interstitials in pure Fe τ is given by (39):

$\tau = 2.92 \times 10^{-15}$ EXP(19800/RT) .

For T = 269.9°K, τ is equal to 0.41 min. which is in agreement with the value of $\tau_{12,1} = 0.523$ min. (see Table 1) obtained for the first stage relaxation.

2. Lognormal Analysis

As was shown in the paper by Nowick and Berry (40), it is more accurate to analyze relaxation processes in terms of a distribution of relaxation times than in terms of single exponentials. Thus, in view of the small mass difference between C_{13} and C_{12}, and consequently in view of the small isotope effect, a further analysis of the relaxation was required:

For a lognormal distribution of the relaxation times the disaccommodation is given by:

$$R = \frac{1}{\mu(\infty)} - \frac{1}{\mu(t)} = \sum_j \frac{a_j}{\sqrt{\pi}} \int_{-\infty}^{\infty} \mathrm{EXP}[-x^2 - \mathrm{EXP}(\ln(t/\tau_{mj}) - \beta_j x)]\, dx \qquad (4)$$

where a_j - relaxation strength of the j^{th} relaxation

β_j - the half width of the Gaussian relaxation time distribution of j^{th} relaxation process

τ_{mj} - the most probable relaxation time of the j^{th} relaxation process

x - dummy variable .

The procedure to obtain a least square fit of the data to Equation (4) was conceptually the same as the one described for the sum of exponential analysis. By comparing the figures in Nowick and Berry's paper with Wert and Zener's results (29), it was concluded that $\beta = 0.6$ would be a proper estimate for the width of the Gaussian relaxation time distribution for the carbon interstitials reorienting in the neighborhood of the Fe-Fe sites. Thus, in fitting the two stage relaxation processes, β_1 was fixed at 0.6 . A best fit was obtained for the ratios $\delta_1 = 1.0366$, $\delta_2 = 1.0069$ with $\beta_2 = 1.0$ as can be seen from Fig. 6 and Table 1..

As will be shown later, the theoretical ratio calculated from reaction rate for the gas mixtures used in this work will be 1.0382 . The discrepency between the above analysis and the theoretical calculation is 0.16% .

3. Lognormal Analysis with Constraint

As the isotope effect of carbon interstitial diffusion is known (35), the lognormal analysis of the data was repeated with the constraint $\delta_1 = 1.0382$ (see below for an explanation of this figure). For this purpose, the two sets of data for Fe-Si-C_{13} and Fe-Si-C_{12} were analyzed simultaneously. The result is shown in Table 1 . As can be seen, the obtained value of $\delta_2 = 1.0077$ differs very little from the value of $\delta_2 = 1.0069$ as obtained from the lognormal analysis without the constraint $\delta_1 = 1.0382$.

Fig. 6

Relative deviation of experimental data of the reluctivity change from calculated curves using the lognormal analysis with various half widths β_2 of the Gaussian relaxation time distribution of the second stage relaxation process

FIG. 6

IV. DISCUSSION

The main question arising in connection with the experimental results concerns the significance of the observed isotope effects of the carbon interstitial reorientation in Fe-Fe sites, δ_1 and particularly in Fe-Si sites, δ_2 .

As has been reviewed in the introduction, the effective mass plays an important role in diffusion. This effective mass is determined by the mass of the diffusing element and the masses of other atoms in the alloys and depends on the correlation of their motions. The results obtained in this work show that δ_1 is different from δ_2 . Thus, following Vineyard's treatment, the effective mass determining the jump rate in the first stage relaxation is different from the effective mass for the second stage relaxation process.

It is known (35) and has been confirmed here that the first stage relaxation is due to the carbon reorientation in the neighborhood of Fe-Fe sites. The isotope effect for this stage can be understood in terms of an Einstein Model, i.e. if only the motion of the carbon interstitial is considered. In this case the effective mass is equal to the real mass leading to a theoretical value of $\delta_1 = 1.0382$ as will be shown below.

As $\delta_2 \neq \delta_1$ while ultimately the same atomic species is diffusing, it is strongly suggested that correlated motion of the diffusing carbon atom and the neighboring

silicon atom affects the effective mass of the carbon. The reasons might be seen in the difference of the binding energies of the Si-C pair and the Fe-C pair. This asymmetric energy distribution may distort the normal potential energy contour of carbon interstitials in Fe-Si sites. Thus, the direction cosines of the angle between the normal of the hyper-surface and the coordinate axes may differ from 1.0 (see Equ. 2).

If only jumps of the diffusing carbon and the correlated motion of the nearest silicon atom (which is not jumping, only moving) are taken into account, the direction cosines of carbon will be $c_C \neq 1.0$ and of silicon $c_{Si}^2 = 1 - c_C^2$ and the direction cosines of all others will be equal to zero. The effective mass of carbon interstitial m^* is then given by $m^* = c_C^2 m_C + c_{Si}^2 m_{Si}$ where m_C, m_{Si} are the real masses of carbon and silicon. Therefore, the ratio of relaxation times of the second stage due to two isotopes C_{13} and C_{12} in this model will be:

$$\delta_2 = \frac{\tau_{13,2}}{\tau_{12,2}} = \frac{\sqrt{m^*_{13}}}{\sqrt{m^*_{12}}} = \sqrt{(c_C^2 m_{C,13} + c_{Si}^2 m_{Si})}/\sqrt{(c_C^2 m_{C,12} + c_{Si}^2 m_{Si})} \qquad (5)$$

For the carbon interstitial jumping in the neighborhood of Fe-Fe sites, the ratio will reduce to $\delta_1 = (m_{C,13}/m_{C,12})^{\frac{1}{2}}$ as $c_C \approx 1.0$, on account of the symmetric distribution of the potential energy contour in the surrounding Fe-Fe-C sites and because of the negligible displacements of iron atoms during the carbon interstitial

jump. The theoretical isotopic masses of C_{13} and C_{12} need to be modified for the methane used in this experiment as the gas carburization mixture consists of neither pure $(CH_4)_{13}$ nor $(CH_4)_{12}$ as stated above. Referring to the gas composition given the modified real mass of C_{13}, $m_{C,13}$ is equal to 12.939 while for C_{12}, $m_{C,12}$ is equal to 12.010 . Therefore, the theoretical ratio for δ_1 is $(12.939/12.010)^{\frac{1}{2}}$ = 1.0382 .

The results of this investigation are in agreement with the above argument as can be seen from Table 1:

The results of lognormal analysis with independent first stage relaxation times, showed that the ratio of the first stage relaxation times was equal to 1.0366, which is 0.16% lower than the theoretical value. The reason for this deviation may be the simplified assumption $c_C \approx 1.0$. It is more likely, however, that temperature fluctuations below the limit of detection are responsible for the deviation.

The ratio of the second stage relaxation times δ_2 is significantly smaller than δ_1 . It varies from 1.0069 to 1.0077 depending on the kind of lognormal analysis performed. The result can be understood formally if it is assumed that $c_C \approx 0.6$ (see Equ. 5). As this cosine represents an angle on a 5 dimensional hyper-surface in phase space, little can be said concerning its physical significance in real space. It might merely be noted that for $c_C \neq 1.0$ the diffusion of a carbon interstitial from one site which

is a nearest neighbor site of a substitutional to an equivilent site must involve the motion of the substitutional, silicon in this case. This appears to be entirely reasonable, if it is recalled that the addition of silicon to iron contracts the iron lattice (41).

V. CONCLUSION

Measurements of the isotope effect of diffusion of C_{13} and C_{12} in a dilute Fe-2.75at%Si alloy demonstrated that 1) carbon interstitials diffusing in the vicinity of Fe-Fe sites behave according to the conventional reaction rate theory, 2) carbon interstitials diffusing in the vicinity of Fe-Si sites show less mass dependence which is due to the correlated motion of the interstitial carbon and the substitutional silicon during the diffusional jump.

REFERENCES

1. Ewing J. A., Magnetic Induction in Iron and Other Metals, London (1892)
2. Snoek J. L., Physica 6, 161,321,591,797 (1939)
3. Snoek J. L., Physica 8, 711 (1941)
4. Snoek J. L., New Developments in Ferromagnetic Materials, Elesvier Publishing Company (1947)
5. Neel L. J., Physique Rad. 12, 339 (1951)
6. Neel L. J., Physique Rad. 13, 249 (1952)
7. Levy P. M., J. Phys. Chem. Solids 76, 415 (1965)
8. VanVleck J. H., J. Chem. Phys. 7, 72 (1939)
9. de Vries G., VanGeest D. W., Gersdorf R. and Rathenan G. W., Physica 25, 1131 (1959)
10. Balthiesen E., Phys. Stat. Solidi 3, 2321 (1963)
11. Hellbardt G., Tech. Mitt. Krupp 18, 25 (1960)
12. Biori G., Ferro A. and Montalentic G., J. Applied Phys. 31, 2121 (1960); 32, 1630 (1961)
13. Brissoneau B. and Moser P., J. Phy. Soc. Jan. 17B-I, 333 (1962)
14. Dietze H. D., Tech. Mitt Krupp 17, 67 (1959)
15. Klein M. V., Phys. Stat. Solidi 2, 881 (1962)
16. Dijkstra L. J. and Sladek R. J., Trans. AIME 197, 69 (1953)
17. Enrietto J. F., Trans. AIME 224, 1119 (1962)
18. Dickenscheid W. and Seemann H. J., Rev. Met. 55, 872 (1958)

19. Gladman and Pickering, J. Iron and Steel Institute 203, 1212 (1965)

20. Ritchie and Rawlings, Acta. Met. 15, 491 (1967)

21. Hampe W. and Widman D., Zs angew. Phys. 15, 360 (1963)

22. Graham R. H., M.S. Thesis, University of Missouri - Rolla (1968)

23. Johnson W. A., Trans. Am. Inst. Mining Met. Engrs. 166, 132 (1946)

24. Lazarus D. and Okkerse B., Phys. Rev. 105, 1677 (1957)

25. Schoren A. H., Phys. Rev. Letters 1, 138 (1958)

26. Chemla M., Ann. Phys. 1, 959 (1956)

27. Pell E. M., Phys. Rev. 119, 1014 (1960)

28. McCracken and Love, Phys. Rev. Letters 5, 201 (1960)

29. Wert C. A. and Zener C., Phys. Rev. 76, 1169 (1949)

30. Vineyard G. H., Phys. Chem. Solids 3, 121 (1957)

31. Rice S. A., Phys. Rev. 112, 804 (1958)

32. Rice S. A. and Nachtrieb N. H., J. Chem. Phys. 31, 139 (1959)

33. Lawson A. W., Rice S. A., Corneliussen R. D. and Nachtrieb N. H., J. Chem. Phys. 32, 441 (1960)

34. Rice S. A. and Frisch H. L., J. Chem. Phys. 32, 1026 (1960)

35. Bosman A. J., Thesis, Amsterdam University (1960)

36. Smith R. P., J. Amer. Chem. Society 70, 2724 (1948)

37. Darken L. S., J. Iron and Steel Inst. 174, 249 (1953)

38. Draper N. R. and Smith H., Applied Regression Analysis, John Wiley & Sons, Inc. New York 276 (1967)

39. Wert C., Phys. Rev. 79, 601 (1950)

40. Nowick A. S. and Berry B. S., IBM Journal, 297 (1961)

41. Lihl F. and Ebel H., Arch. Eisenhuttenw 32, 489 (1961)

VITA

Edward T. Yen was born on May 19, 1941, in Shanghai, China. He entered the Taiwan Cheng Kung University in 1962 and graduated in 1965 with the degree of Bachelor of Science in Metallurgical Engineering.

He has been enrolled in the Graduate School of The University of Missouri - Rolla since September, 1966.

APPENDIX

```
C
C      LOGNORMAL ANALYSIS
C
C      PROGRAMMED BY EDWARD T. YEN
C     *NOTES AT THE END OF THIS PROGRAM
C
C     MAINLINE
C
       DIMENSION T(100),PHI(100),FARAD(100),P(4),
      1 PHR(100),R(100),A(10,10),B(10),AA(20),
      2 XEPS(4),X95CON(4),RES(100),CAL(100),FK(100),
      3 PERC(100),DER(4,100)
       COMMON SPI,T,R,P,N,NP
       SPI = 1.772454
C
C      INPUT
C
C      READ IN: N DATA, TRIPLETS T,PHI,FARAD;INITIAL
C      GUESSES P AND ERROR LIMIT EPS
C
       N = NN
       READ (1,31) NN,RO
    31 FORMAT (7X,I2,  / F 10.1)
       DO 42 J=1,NN
       READ  ( 1,41)  I,    T(J),PHI(J), FARAD(J)
    41 FORMAT (I3,F17.2,2F20.2)
    42 CONTINUE
        NP = 4
       READ (1,77) (P(I),I = 1,NP)
    77 FORMAT (4E18.8)
       READ (1,88) EPS
    88 FORMAT ( 7X,F8.4)
C
C      RELUCTIVITY CALCULATION
C
C      ADAPT INPUT DATA TO NUMBERS PROPORTIONAL TO
C      PERMEABILITY, REFERENCE PARALLEL RESISTOR
C      ASSUMED TO 1.0 KOHMS
C
       DO 2000  K=1,NN
 2000 PHR(K)=(FARAD(K)*50.*(1000.+(PHI(K)*10.))/
     1 (1000.+(PHI(K)*10.)+50.)) -RO
       DO 2005   K=1,NN
 2005 PHI(K)=1./PHR(K)
       DO 2008  K=1,NN
 2008    R(K)=(PHI(NN)-PHI(K) )*1.0E+07
       WRITE (3,999)
  999 FORMAT (1H1, 7X,3H I ,10X,5H T   ,14X,5H R    /)
       DO 333 I=1,NN
       WRITE  (3, 777) I,T(I), R(I)
  777 FORMAT  (7X, I3, 2E20.4 )
  333 CONTINUE
```

```
C
C       ITERATION
C
        BETA = .0
 1007 CONTINUE
        SWITCH = .0
        L=1
  100 DO 103 NA = 1,N
C       BUILD NORMAL EQUATIONS
        CALL FNK (NA,BETA,XFK)
        FK(NA) = XFK
        DO 103 K = 1,NP
        CALL DERFNK ( NA , BETA,XDER,K)
  103   DER ( K,NA) = XDER
C       SET UP MATRIX
        DO 666 K = 1,NP
        B(K) = 0.0
        DO 104 NA = 1, N
  104   B(K) = B(K) + ( R(NA) - FK(NA))* DER(K,NA)
  666 CONTINUE
        DO 105 K = 1,NP
        DO 105 J = K,NP
        A(K,J) = .0
        DO 106 NA= 1,N
  106 A(K,J) = A(K,J) + DER(K,NA) * DER (J,NA)
  105   A(J,K) = A(K,J)
        IF (SWITCH) 30,33,30
   33   CONTINUE
        DO 13 K = 1,NP
        DO 13 J = 1,NP
        IF (K-1) 8,7,8
    7   AA(J) = A(J,K)
        GO TO 13
    8   IF (K-2) 10,9,10
    9   AA(J+4) = A(J,K)
        GO TO 13
   10   IF (K-3 ) 12,11,12
   11   AA(J+8) = A(J,K)
        GO TO 13
   12   AA (J+12) = A (J,K)
   13   CONTINUE
C       SOLVE NORMAL EQUATIONS
        CALL SIMQ (AA,B,NP ,KS)
        IF (IABS(KS)) 14,15,14
   14   WRITE (3,90)
   90   FORMAT  (1X,18HMATRIX IS SINGULAR )
        CALL EXIT
   15   CONTINUE
        XXEPS = .0
C       ADJUST PARAMETERS
        DO 16 K = 1,NP
        XEPS (K) = B(K) / P(K)
```

```
      P(K) = P(K) + B(K)
   16 XXEPS = XXEPS + XEPS (K)**2
C     TEST FOR CONVERGENCE
      IF (EPS - ABS ( SQRT ( XXEPS ))) 38,300,300
  300 SWITCH = 1.
      GO TO 100
   38 CONTINUE
C     INTERMEDIATE OUTPUT
      IF ( L-1) 20,201,20
  201 WRITE (3,202)
  202 FORMAT (1H1,12X,19HINTERMEDIATE OUTPUT  )
   20 WRITE(3,101)
  101 FORMAT (1X,/////)
      WRITE (3,53) (I,I=1,NP)
   53 FORMAT ( 5H ITER,4(7X,2HP(,I1,1H),3X))
      WRITE (3,52)  L,(P(I),I=1,NP)
   52 FORMAT (2X,I2,3X,1P4E14.6///)
      L = L+1
      GO TO 100
C
C     VARIANCE ,CONFIDENCE LIMIT, RESIDUALS AND
C     PERCENT DEVIATION CALCULATIONS
C
   30 CALL CONF(   BETA, X95CON,A,VAR,FK)
      DO 40  K= 1,N
      CAL(K) = FK(K)
      RES(K) = R(K) - CAL(K)
   40 PERC(K) = RES(K)/R(K)
C
C     OUTPUT
C
      WRITE (3,61)
   61 FORMAT (1H1, 14X , 15H FINAL RESULTS   //)
      WRITE (3,62)
   62 FORMAT (15X,10HPARAMETER,11X,10HCONF.LIMIT  /)
      WRITE (3,63) P(1),X95CON(1)
      WRITE (3,64) P(2),X95CON(2)
      WRITE (3,65) P(3),X95CON(3)
      WRITE (3,66) P(4), X95CON (4)
      WRITE (3,67) BETA
      WRITE (3,68) VAR
      WRITE (3,69) EPS
   63 FORMAT ( 5X , 10H R1     =        ,1PE14.7,3X,
     1 1H*,1X,E14.7)
   64 FORMAT ( 5X , 10H R2     =        ,1PE14.7,3X,
     1 1H*,1X,E14.7)
   65 FORMAT ( 5X , 10H T1     =        ,1PE14.7,3X,
     1 1H*,1X,E14.7)
   66 FORMAT ( 5X , 10H T2     =        ,1PE14.7,3X,
     1 1H*,1X,E14.7)
```

```
   67 FORMAT ( 5X , 10H BETA   =         ,F14.7)
   68 FORMAT ( 5X , 10H VAR    =         ,1PE14.7)
   69 FORMAT ( 5X , 10H EPS    =         ,1PE14.7)
      WRITE (3,71)
   71 FORMAT (//// 7X,2H I,15X,4HTIME,10X,4HPERM,
     1 14X,8HOBSERVED,9X,11H CALCULATED ,9X,
     2 9HRESIDUAL ,9X,10H DEVIATION     //)
      DO 1000 I = 1,N
      WRITE (3,72)  I,  T(I), PHI(I),P(I),CAL(I),
     1 RES(I),PERC(I)
   72 FORMAT(7X,I3,6E18.4)
 1000 CONTINUE
        IF ( BETA-2.0 ) 1009,1005,1005
 1009 BETA = BETA + .20
      GO TO 1007
 1005 CONTINUE
      STOP
      END
C
      SUBROUTINE FNK ( NA,BETA, EX)
C
      EXTERNAL FCT1,FCT2,FCT3,FCT4
      DIMENSION P(4),T(100),R(100)
      COMMON SPI,T,R,P,N,NP
      ZETA = 0.6
      CALL W1QH10  (FCT1,NA,ZETA,XINT )
      CALL W1QH10 ( FCT3,NA,BETA,YINT)
      EX = (P(1) *XINT + P(2) * YINT ) / SPI
      RETURN
      END
C
      SUBROUTINE DERFNK ( NA,BETA,EX,K)
C
      EXTERNAL FCT1,FCT2,FCT3,FCT4
      DIMENSION P(4),T(100),R(100)
      COMMON SPI,T,R,P,N,NP
      ZETA = 0.6
      IF (K-1) 2,1,2
    1 CALL W1QH10  (FCT1,NA,ZETA,XINT )
      EX = XINT / SPI
      GO TO 100
    2 IF (K-2) 4,3,4
    3 CALL W1QH10 ( FCT3,NA,BETA,YINT)
      EX = YINT/SPI
      GO TO 100
    4 IF (K-3) 6,5,6
    5 CALL W1QH10  (FCT2,NA,ZETA,XINT )
      EX =(P(1) / SPI)* XINT*(T(NA)/ P(3) **2)
      GO TO 100
    6 CALL W1QH10 ( FCT4,NA ,BETA,YINT)
      EX =(P(2) / SPI)* YINT*(T(NA)/ P(4) **2)
  100 RETURN
      END
```

```
C
      FUNCTION FCT1 ( NA,ZETA,U)
C
      DIMENSION P(4),T(100),R(100)
      COMMON SPI,T,R,P,N,NP
      C = EXP (-ZETA*U)
      FCT1 = EXP (-T(NA)/P(3) *C )
      RETURN
      END
C
      FUNCTION FCT2 ( NA,ZETA,U)
C
      DIMENSION P(4),T(100),R(100)
      COMMON SPI,T,R,P,N,NP
      D = EXP (-ZETA*U)
      FCT2 = EXP (-T(NA)/P(3) * D - ZETA*U )
      RETURN
      END
C
      FUNCTION FCT3 ( NA,BETA,U)
C
      DIMENSION P(4),T(100),R(100)
      COMMON SPI,T,R,P,N,NP
      C = EXP (-BETA*U)
      FCT3 = EXP (-T(NA)/P(4) *C )
      RETURN
      END
C
      FUNCTION FCT4 ( NA,BETA,U)
C
      DIMENSION P(4),T(100),R(100)
      COMMON SPI,T,R,P,N,NP
      D = EXP (-BETA*U)
      FCT4 = EXP (-T(NA)/P(4) * D - BETA*U )
      RETURN
      END
C
      SUBROUTINE W1QH10 ( FCT,NA,BETA,Y)
C
      DIMENSION P(4),T(100),R(100)
      X = 3.436159
      Z = -X
      Y = .7640433 E-05 * ( FCT(NA,BETA,X)+
     1 FCT(NA,BETA,Z))
      X = 2.532732
      Y = Y +.134364E-02* ( FCT(NA,BETA,X) +
     1 FCT(NA,BETA,Z))
      X = 1.756684
      Z = -X
      Y=Y+.338744E-01    * ( FCT(NA,BETA,X) +
```

```
     1 FCT(NA,BETA,Z))
       X = 1.036611
       Z = -X
       Y = Y + .2401386  * ( FCT(NA,BETA,X) +
     1 FCT(NA,BETA,Z))
       X = .3429013
       Z = -X
       Y = Y + .6108626  * ( FCT(NA,BETA,X) +
     1 FCT(NA,BETA,Z))
       RETURN
       END
C
       SUBROUTINE CONF ( BETA,X95CON,A,VAR,XEX)
C
       DIMENSION P(4),T(100),R(100),X95CON(4),
     1 A(10,10),X(10),Y(10),I(10),J(10),XEX(100)
       COMMON SPI,T,R,P,N,NP
       ND = 10
       EPS = .001
       VAR = .0
       DO 10 K = 1,N
    10 VAR = VAR + (R(K) - XEX(K) ) **2
       DF = N - 3
       VAR1 = VAR / DF
       TFACT = (1.96*DF+.60033+.9591/DF)/(DF-.90259
     1 +.11588/DF)
       CALL INVRT (A,ND,NP,EPS,DEL,X,Y,I,J,KEY)
       DO 11 K = 1,NP
    11 X95CON (K) = TFACT * SQRT(A(K,K)* VAR1)
       RETURN
       END
```

```
C
C       NOTES
C
C       IN THIS PROGRAM FOLLOWING TERMS ARE USED AS
C       EX -- THE MAIN FUNCTION SERVED FOR LOGNORMAL
C             ANALYSIS CALCULATION
C       PHR -- SUBSIDAEY FUNCTION FOR PERMEABILITY
C              CALCULATION
C       R -- RELUCTIVITY CHANGE
C       FARAD -- OBSERVED FARAD FARAD IN A.C. BRIDGE
C       RO -- REFERENCE PERMEABILITY
C       T -- TEMPERATURE
C       PHI -- OBSERVED SCALE ON THE RECORDER CHART
C       P -- PARAMETERS IN ESTIMATION
C       EPS -- ERROR LIMIT
C       N -- NUMBER OF DATA POINTS
C       NP -- NUMBER OF PARAMETERS
C       X95CON -- 95 PERCENT CONFIDENCE LIMIT
C       RES -- RESIDUALS
C       CAL -- CALCULATED RELUCTIVITY CHANGE
C       PERC -- PERCENTAGE DEVIATION
C       DER -- DERIVATIVE OF THE FUNCTION FK
C       VAR -- VARIANCE
C       SPI -- INVERSE SQUARE ROOT OF PIE
C       BETA,ZETA -- VARIABLES
```